

Mode-coupling theory predictions for a limited valency attractive square well model

This article has been downloaded from IOPscience. Please scroll down to see the full text article.

2006 J. Phys.: Condens. Matter 18 S2373

(<http://iopscience.iop.org/0953-8984/18/36/S11>)

View [the table of contents for this issue](#), or go to the [journal homepage](#) for more

Download details:

IP Address: 129.252.86.83

The article was downloaded on 28/05/2010 at 13:30

Please note that [terms and conditions apply](#).

Mode-coupling theory predictions for a limited valency attractive square well model

E Zaccarelli^{1,2}, I Saika-Voivod³, A J Moreno⁴, E La Nave^{1,2},
S V Buldyrev⁵, F Sciortino¹ and P Tartaglia⁶

¹ Dipartimento di Fisica and CNR-INFM-SOFT, Università di Roma 'La Sapienza', Piazzale Aldo Moro 2, I-00185, Roma, Italy

² ISC-CNR, Via dei Taurini 19, I-00185, Roma, Italy

³ Department of Chemistry, University of Saskatchewan, Saskatoon, Saskatchewan, S7N 5C9, Canada

⁴ Donostia International Physics Center, Paseo Manuel de Lardizabal 4, E-20018 San Sebastián, Spain

⁵ Department of Physics, Yeshiva University, 500 W 185th Street, New York, NY 10033, USA

⁶ Dipartimento di Fisica and CNR-INFM-SMC, Università di Roma 'La Sapienza', Piazzale Aldo Moro 2, I-00185, Roma, Italy

E-mail: emanuela.zaccarelli@phys.uniroma1.it

Received 31 January 2006, in final form 28 March 2006

Published 24 August 2006

Online at stacks.iop.org/JPhysCM/18/S2373

Abstract

Recently we have studied, using numerical simulations, a limited valency model, i.e. an attractive square well model with a constraint on the maximum number of bonded neighbours. Studying a large region of temperatures T and packing fractions ϕ , we have estimated the location of the liquid–gas phase separation spinodal and the loci of dynamic arrest, where the system is trapped in a disordered non-ergodic state. Two distinct arrest lines for the system are present in the system: a (*repulsive*) *glass* line at high packing fraction, and a *gel* line at low ϕ and T . The former is essentially vertical (ϕ controlled), while the latter is rather horizontal (T controlled) in the $(\phi-T)$ plane. We here complement the molecular dynamics results with mode coupling theory calculations, using the numerical structure factors as input. We find that the theory predicts a repulsive glass line—in satisfactory agreement with the simulation results—and an attractive glass line, which appears to be unrelated to the gel line.

(Some figures in this article are in colour only in the electronic version)

1. Introduction

In recent years, investigation of structural arrest in colloidal systems has witnessed a renewed and large interest in the scientific community since new phenomena have been identified, in particular when the particles interact via an attractive potential of range short enough compared

to the size of the colloid [1]. Theoretical [2–4], numerical [5–7] and experimental [8–13] studies have shown the existence of two different mechanisms responsible for the slowing down characteristic of structural arrest. At high temperature T and high packing fractions ϕ of the dispersed phase, caging effects prevail and produce the typical repulsive glass behaviour. At low T , and slightly smaller ϕ , another mechanism sets in, due to the stickiness of the particles, and generates a so-called attractive glass [14]. It was hypothesized at the beginning that the latter mechanism could be one of the routes to the formation of a gel at low densities [3]. Many investigations of these phenomena have been made [15, 16], but most of them were faced with difficulties related to the existence of a two-phase region at low ϕ . In fact it was unambiguously shown, for the case of short-range attractive potentials, that the arrest line intersects the binodal line at its high-volume-fraction side [17, 18]. The crossing may be avoided if a lowering and shrinking of the two-phase coexistence region is achieved.

One possibility to limit or suppress phase separation is to consider the effects of a long-range repulsion complementing the short-range attraction. This type of potential, able to mimic effects of screened electrostatic interactions, properly describes interactions in charged colloidal suspensions. This route has been actively pursued very recently in experiments [19–21], simulations [22–26] and theory [27–30].

Another possibility to limit or suppress phase separation, which does not invoke the presence of repulsive long-range repulsion, is offered by saturation of bonding, i.e. by a limit on the maximum number of bonded interactions. To prove this mechanism, we have devised a model where an ad hoc constraint is adopted, in addition to a square well (SW) interaction. We studied numerically a saturated SW model first introduced by Speedy and Debenedetti [31, 32]⁷, also named the limited valency model. In this model, the square well attraction between two particles is constrained to a maximum number of bonds n_{\max} that particles can form. By reducing n_{\max} to low values such as 3, 4, 5, we found that the location of phase separation is progressively shrunk both in ϕ and T [33]. Hence, reduction in the number of bonds may avoid the crossing between the dynamic arrest and the binodal lines, or move the crossing to much lower ϕ and T . Simulating this model, we showed that indeed the avoidance of phase separation allows the emergence of arrested states at low ϕ , which have quite different physical features than glasses, both of attractive and repulsive type. Completing the study up to very large densities in [34], we detected the presence of two distinct arrest lines: a gel line, practically flat in T , governed by Arrhenius dynamics, and a glass line, practically constant in ϕ , corresponding to the standard hard sphere glass transition. All along the gel line, the dynamic features are not reducible to those of attractive glasses, suggesting that the two states in attractive systems do not necessarily correspond to the same phenomenon, and a simple extension of the attractive glass line may not be always appropriate.

The purpose of the present work is to use the MCT in order to check the conclusions obtained through numerical simulations, to clarify in particular the possibility of describing the low ϕ equilibrium gel formation. To this aim, we compare here our numerical results of references [33, 34] with predictions of mode coupling theory (MCT) for the same model, using as input of the theory the ‘exact’ structure factors for the n_{\max} model, calculated numerically.

2. Overview of the simulation results

The limited valency model described above has been recently studied in detail and we summarize here the main results of the numerical investigation [33, 34]. Molecular dynamics was performed in a square well attractive system of $N = 10^4$ particles of unit mass and hard

⁷ However, differently from [31, 32], we do not impose any constraint on minimal bonded loops.

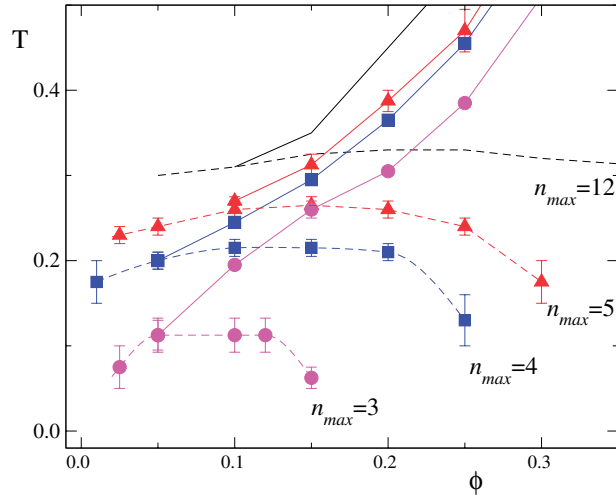


Figure 1. Spinodal and percolation lines (dashed and solid lines respectively) of the limited valency model for $n_{\max} = 3$ (circles), $n_{\max} = 4$ (squares), $n_{\max} = 5$ (triangles) and $n_{\max} = 12$ (no symbols).

core $\sigma = 1$ with a range of the well Δ such that $(\sigma + \Delta)/\sigma = 1.03$ and depth u_0 . Temperature is measured in units of u_0 , with the Boltzmann constant $k_B = 1$. The maximum number of bonds was limited to $n_{\max} = 3, 4, 5$ as compared to the unconstrained SW, where $n_{\max} = 12$. Indeed, for $n_{\max} > 6$, no significant difference in the phase behaviour was observed with respect to the standard square well model. The main findings are reported in the following list summarizing our results.

- (i) The coexistence region in the (ϕ, T) plane reduces in size as n_{\max} decreases; the values of ϕ above which the spinodal disappears are $\phi \approx 0.20$ and $\phi \approx 0.30$ for $n_{\max} = 3$ and 4 respectively. The loci of percolation also shift to lower T values, and cross the two-phase region on the low ϕ side, as shown in figure 1.
- (ii) The bonds formed due to the attraction show a lifetime which follows an Arrhenius behaviour in T .
- (iii) The mean squared displacement develops a plateau at low T which defines a localization length of the order of the particle size, much larger both than the length typical of a repulsive glass due to caging (of the order of 0.1σ) and than that of an attractive glass (of the order of the well width). The diffusivity shows a power-law behaviour in ϕ along constant temperature paths, while it displays an Arrhenius dependence on T for constant volume fraction.
- (iv) The normalized intermediate scattering functions show a corresponding plateau at low T only for values of the momentum transfer q smaller than the value corresponding to the first peak of the structure factor. This feature is rather different from the standard behaviour close to a glass transition, and is similar to the behaviour of a chemical gel [35].
- (v) The height of the plateau for the normalized intermediate scattering functions, i.e. the non-ergodicity factor f_q , has a different shape in q for the gel than both its attractive and repulsive glass counterparts.

Based on these facts we concluded that the system shows a *glass* line at high ϕ and a *gel* line at low T and low ϕ . More important, the dynamical behaviour observed close to the gel line does not seem to allow the identification of the gel with the attractive MCT glass.

3. Mode coupling theory

We solve the MCT equations to locate the ideal glass line(s) in the $(\phi-T)$ plane. The MCT, starting only from the structural information contained in the static structure factor $S(q)$, provides indication of the onset of non-ergodic behaviour [36]. Although the theory is not strictly based on the hypothesis of pair additivity for the interaction potential, its main (uncontrolled) approximation is the factorization of higher-order correlation functions into products of pair correlation functions [36, 37]. Since the n_{\max} model incorporates many-body terms in the Hamiltonian [33, 34], we cannot expect the theory to work at its best. Perhaps higher-order correlations should also be considered, as in the case of silica, a tetrahedral network-forming liquid, where the triplet correlation function c_3 provides a relevant contribution to the MCT kernel [38]. Here, we limit ourselves to the standard version of MCT calculation, because the random nature of the n_{\max} bonds along the particle surface does not produce any angular constraint, retaining the full sphericity for the model. However, it would be interesting to check in a future work whether the inclusion of the corresponding three-point correlators calculated within MD simulations produces any significant difference in the MCT results.

MCT is able to predict the full time evolution for the density–density autocorrelation function $\Phi(q, t)$ as a function of the momentum transfer q and t , through coupled non-linear integro-differential equations. For a given interaction potential, through the knowledge of $S(q)$, the memory kernel entering the nonlinear term of the MCT equations can be evaluated and the equation solved for various values of q . In particular, the non-ergodicity transition leading to structural arrest is obtained by performing the limit $t \rightarrow \infty$ in the equations. Defining the non-ergodicity factor as the long-time limit of Φ correlator $\lim_{t \rightarrow \infty} \Phi(q, t) = f(q)$, $f(q)$ is found to be the solution of [36],

$$\frac{f(q)}{1 - f(q)} = m(q) \quad (1)$$

where the memory kernel $m(q)$ is quadratic in the correlator itself,

$$m(q) = \frac{1}{2} \int \frac{d^3k}{(2\pi)^3} \mathcal{V}(\mathbf{q}, \mathbf{k}) f(k) f(|\mathbf{q} - \mathbf{k}|). \quad (2)$$

The vertex functions \mathcal{V} , the coupling constants of the theory, are

$$\mathcal{V}(\mathbf{q}, \mathbf{k}) = \frac{\rho}{q^4} [\mathbf{q} \cdot (\mathbf{q} - \mathbf{k}) c(|\mathbf{q} - \mathbf{k}|) + \mathbf{q} \cdot \mathbf{k} c(k)]^2 S(q)S(k)S(|\mathbf{q} - \mathbf{k}|) \quad (3)$$

and depend only on the Fourier transform of the direct correlation function $c(q)$, or equivalently on $S(q)$, and on the number density ρ . In the A_2 bifurcation scenario of MCT [36] the solutions of equation (1) jump from zero to a finite value at the ideal glass transition. The locus of the fluid–glass transition can be calculated varying the control parameters of the system, ϕ and T . For a square well model, there is an additional control parameter, that is the range of attraction Δ . In this case, higher order bifurcations of the solutions arise when $\Delta < \Delta^* \sim 0.041$ [4]. In this case, two distinct glassy solutions appear, a repulsive and an attractive glass respectively, with different non-ergodicity parameters and mechanical properties [39].

We calculate the MCT ideal glass transition line for $n_{\max} = 3$ using as input the numerical $S(q)$, ‘exact’ within numerical precision. In the evaluation of the MCT kernel of equation (2), it is crucial to integrate over all q contributing to the memory function. For short-range attractive potentials, it is important to integrate up to very large q values, since the information of the potential shape is coded into the large q region. From a numerical point of view, it is convenient to evaluate $S(q)$ at large q by Fourier transforming the pair distribution function $g(r)$, and at

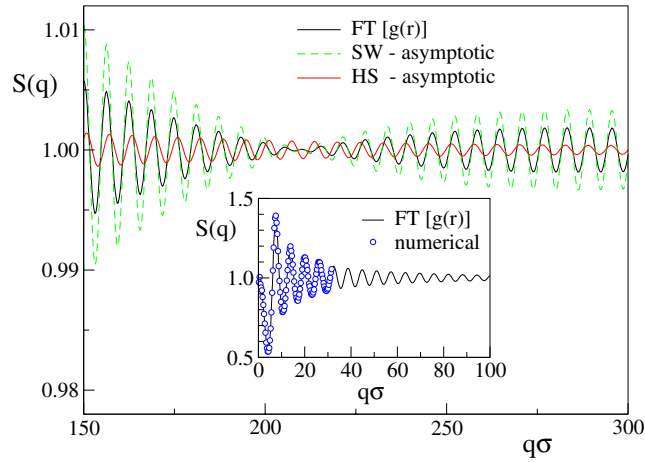


Figure 2. Inset: static structure factor for $\phi = 0.20$ and $T = 0.2$ used as input in MCT calculated directly from simulations (points), and by Fourier transform of the $g(r)$ (line). Main: enlargement of the large- q behaviour displaying ‘beats’. For comparison we also report the corresponding asymptotic SW (differing only by a factor A in amplitude) and HS (out of phase) results.

small q by direct evaluation of $S(q)$ in q -space. Indeed, bonding in $g(r)$ is reflected by a very large and constant signal between σ and $\sigma + \Delta$, which fully accounts for the large- q behaviour of $S(q)$. For the same reason, the large- q ‘beats’ [40] in $S(q)$ have the same shape as the standard SW and carry information on the short-range potential. The asymptotic form of $S(q)$ for large q , both for the SW and the n_{\max} model, is

$$S_{\text{asympt}}(q) = 1 - \frac{A}{q^3} \{ \sin(q\sigma) - q\sigma \cos(q\sigma) + (e^{\beta u_0} - 1)[q(\sigma + \Delta) \cos(q(\sigma + \Delta)) - \sin(q(\sigma + \Delta)) + \sin(q\sigma) - q\sigma \cos(q\sigma)] \}. \quad (4)$$

The amplitude A (which depends on T and ϕ) is different for the SW and n_{\max} models, being smaller in the n_{\max} case, due to the reduced number of bonded neighbours. Combining information from $S(q)$ and $g(r)$, an accurate description of $S(q)$ over the entire relevant q range is obtained, as shown in figure 2. In the SW case, the large- q oscillations resulting from the narrow width of the square well potential are largely responsible for the MCT attractive glass transition [4]. We solve the MCT equations in q -space in the window from 0 to $600\sigma^{-1}$, with a mesh of about $0.3\sigma^{-1}$, for a total of 2000 q -vectors. We bracket the MCT arrest line by locating two adjacent state points along isochores where a liquid and glassy solutions are respectively found. The resulting MCT predictions are reported in figure 3.

At high densities, MCT results are very similar to those found for the simple SW [4, 39] for the $\Delta = 0.03$ case. Even in the n_{\max} case, the MCT equations predict two distinct glass lines, respectively an attractive and a repulsive one, and a glass–glass transition ending in an A_3 singularity [41]. A comparison between the MCT predictions for the SW and for the n_{\max} model is reported in figure 3. The glass lines for both models converge to the hard-sphere result at high T and to the same locus for $\phi \rightarrow 0$. This is consistent with the expectation that at high ϕ arrest is driven by packing, while at low ϕ the constraint on the maximum number of bonded neighbours becomes irrelevant and hence the two models tend to become similar. Differences with respect to the SW case are observed at intermediate ϕ .

In the SW case the ideal MCT attractive glass line is rather flat, monotonically decreasing in T , almost merging into the spinodal on the left side of the critical point [39]. The n_{\max} model

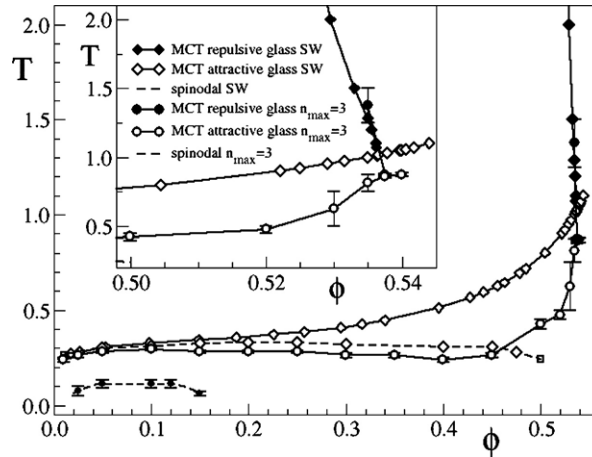


Figure 3. Comparison of MCT predictions and spinodal lines for the SW case and for the n_{\max} model with $n_{\max} = 3$. The inset shows an enlargement of the high- ϕ region, to visualize the attractive and repulsive lines and the glass-glass transition.

shows instead a non-monotonicity of the T -dependence of the attractive line with decreasing ϕ , causing the presence of a minimum in T for $\phi \approx 0.4$ and $T \approx 0.24$. The significant suppression of the attractive glass line in the n_{\max} model at intermediate ϕ arises from the decrease in the number of bonded nearest neighbours as compared to the SW case. The attractive glass line has a maximum around $\phi \approx 0.10$ and $T \approx 0.3$, before turning down following the spinodal as in the SW case, on the left of the critical point. It is possible that the shape for $\phi \lesssim 0.1$ in the MCT line is an echo of the underlying increase of the compressibility at low ϕ due to the close-by spinodal, since at low ϕ the MCT line roughly follows in shape the loci of constant $S(0)$ (see figure 6).

In the SW, the attractive and the repulsive glass lines differ essentially in the q -dependence of the non-ergodicity parameter f_q . The theory also allows us to calculate f_q and its critical value at the glass transition. As compared to the repulsive glass, the attractive glass is characterized by much larger f_q values, extending to much larger q . These features are also displayed in the theoretical calculations for the n_{\max} model. Along the attractive glass line, for all ϕ values, from about $\phi = 0.05$ up to $\phi = 0.54$, the critical non-ergodicity parameter, i.e. f_q at the MCT transition, does not change significantly. Figure 4 shows the full q -vector dependence for both types of glasses. We have also verified that in the attractive glass phase f_q is significantly dependent on T .

For comparison, we plot in figure 5 the non-ergodicity parameters estimated from the simulations, via a stretched exponential fit of the ϕ correlators [34], along the iso-diffusivity line $DT^{-1/2} = 0.0005$. A transition from a gel to a glass is evident. However, the shape of f_q never resembles that of an attractive glass. The gel is characterized by non-ergodic features only at large length-scales, due to the mobility of the network in the available free space, while an attractive glass is strictly confined within the bond length. The main difference between theoretical and simulation results is that, although also in the gel bonds are on average permanent on the timescale of the simulations at low T [34], the limited number of neighbours accounts for residual motions of the particles. Hence, particles are confined by the attractive well width only relative to each other, but still can freely explore up to their diameter length without ever breaking the network. In the theoretical calculations, however, the presence of the short-range bonds, manifested in the large- q tail of $S(q)$, is responsible for the non-ergodic transition.

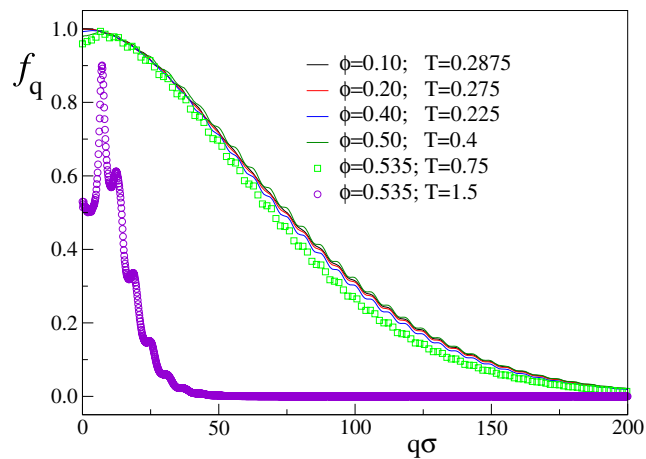


Figure 4. Critical non-ergodicity parameters f_q calculated within MCT. Note that at low ϕ along the attractive glass line the f_q are indistinguishable.

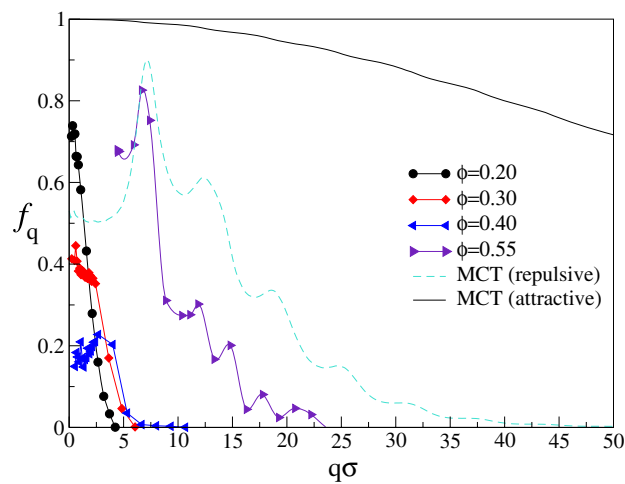


Figure 5. Critical non-ergodicity parameter f_q calculated from the simulations (i.e. along the iso-diffusivity line $DT^{-1/2} = 0.0005$), via a stretched exponential fit of the ϕ correlators. Note that f_q never resembles that of an attractive glass. Lines are guides to the eye.

Already at the SW level, the theory strongly overestimates the tendency to form an attractive glass [42, 43]. Compared with numerical simulation [44], the theoretical attractive glass line has to be shifted approximatively by a factor of three to four in T , while the repulsive glass line needs only a 10% adjustment in ϕ . The correction of the location of the ideal MCT lines provokes a major effect: the attractive glass line does not lie above the critical point but meets the spinodal at low T on the right side [17]. If the overestimate of the attractive glass line is properly taken into account, then one has to conclude that it is not possible to form arrested states at low ϕ without the intervention of a phase separation. Recent simulation studies confirm that this is the case independently from the width of the attraction range [18]. It is also necessary to recall that the ideal MCT glass lines, especially when energetic caging is dominant, have to be interpreted as cross-over lines, from a power law to an activated dependence of dynamic

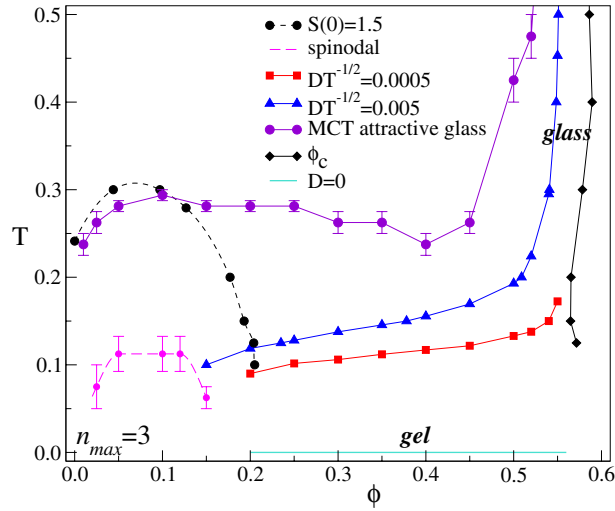


Figure 6. Summary of the thermodynamic and kinetic phase diagram for $n_{\max} = 3$, including spinodal (dashed lines with filled circles), iso-diffusivity loci where $D/\sqrt{T} = 0.005, 0.0005$ (lines with triangles and squares), iso- $S(0)$ locus where $S(0) = 1.5$, MCT lines (attractive and repulsive), extrapolated *glass*, labelled as ϕ_c , and *gel*, labelled as $D = 0$, lines respectively from power law and Arrhenius fits ($T_c = 0$) [34].

properties [45]. We can summarize the dynamical arrest behaviour in figure 6. One locus of arrest is found at high ϕ , rather vertical and corresponding to the hard-sphere glass transition. This locus is quite well described by MCT. Very different is the situation concerning the low T slowing down. The isodiffusivity lines suggest a rather flat arrest line. Two different loci could be associated with arrest at low T : one defined by the T_c of the power-law fits of the diffusivity and one at $T = 0$ associated with the vanishing of D according to the Arrhenius law [34]. It would be tempting to associate the T_c -line with the attractive glass line predicted by MCT and interpret the wide region between the two lines as a region of activated bond-breaking processes [42].

Results for the present model provide evidence that a gel line cannot necessarily be considered an extension of the attractive glass line. Here, a gel never transforms into an attractive glass, but only into a repulsive glass with increasing ϕ . The competition between the two arrested states seems also to produce anomalies in the dynamics of the same kind as those found in the presence of MCT higher-order singularities [34]. In particular, these anomalies correspond to a logarithmic relaxation for the density correlators in the liquid region close to the singularity, accompanied by a sub-diffusive behaviour for the mean squared displacement [44].

4. Conclusions

The aim of this work was to compare results for the dynamical arrest in the n_{\max} model for $n_{\max} = 3$ with MCT predictions. Using the numeric $S(q)$, ‘exact’ within the precision of the statistical averages, we have solved the MCT equations and evaluated the glass lines. The theoretical results differ only slightly from the SW case and do not provide any indication of a gel line. According to the theory an attractive glass line (i.e. with the typical features of the attractive glass as localization length $\sim \Delta^2$ and very wide f_q) should be present. From a

theoretical point of view, such a line arises from the large- q oscillations in $S(q)$, i.e. from the q -space signature of the short-range bonding. Hence, it has the same origin as in the SW. In the simulation of the n_{\max} model the bond localization is not observed, either in the MSD or in the width of f_q . We believe this is due to the fact that, although bonding is present, particles are confined by the potential well only relative to each other. Indeed, at low ϕ , oscillations of parts of the connected network are possible, preventing the observation of the MCT mechanism for arrest. At small ϕ , even at extremely low T , when the bond lifetime becomes comparable to the simulation time and bonds between particles are essentially permanent, it was shown in [34] that the plateau of the MSD remains of the order of the particle size. Of course, the inclusion in the MCT calculation of higher-order correlation functions could be important in the study of a many-body interaction and should be considered. However, due to the sphericity of the model, our opinion is that this should not make a significant change, i.e. the prediction for the attractive glass transition should be robust in this respect.

In summary, the present study provides a clear indication that in the present model, where the liquid–gas phase separation can be avoided and arrest at low ϕ can be explored in equilibrium conditions, the observed arrested state is substantially different from the the low- ϕ extension of the attractive glass. In the present model, in which bonding interactions are not strongly directionally constrained, large amplitude motions are possible within the fully bonded network. These modes significantly affect the shape of the correlation functions and make it impossible to observe the short-range localization characteristic of the attractive glass.

The comparison with the solution of the MCT equations for the n_{\max} model (a possibility offered by the spherical symmetry of the interaction potential) confirms that MCT significantly overestimates the role of the bonding, predicting an attractive glass even in the present case. The present results strongly suggest that the attractive glass is an arrested state of matter which can be observed in short-range attractive potentials only at relatively high ϕ , being limited by the spinodal curve. When the inter-particle potential favours a limited valency, arrest at low ϕ in the absence of phase separation becomes possible but with a mechanism based on the connectivity properties of the particle network. The dynamic features of this slowing down, at least in this model of geometrically uncorrelated bonds, are clearly different from what would be the extension of the (attractive) glass line.

Acknowledgments

FS and PT acknowledge with pleasure the collaboration with Sow-Hsin Chen in the course of various years, and dedicate this work to the celebration of his 70th birthday. We acknowledge support from MIUR-Cofin, MIUR-Firb and MRTN-CT-2003-504712. IS-V acknowledges NSERC (Canada) for funding. We thank W Kob for useful discussions.

References

- [1] Sciortino F and Tartaglia P 2005 *Adv. Phys.* **54** 471
- [2] Fabbian L, Götze W, Sciortino F, Tartaglia P and Thiery F 1999 *Phys. Rev. E* **59** 1347–50
- [3] Bergenholtz J and Fuchs M 1999 *Phys. Rev. E* **59** 5706–15
- [4] Dawson K A, Foffi G, Fuchs M, Götze W, Sciortino F, Sperl M, Tartaglia P, Voigtmann T and Zaccarelli E 2001 *Phys. Rev. E* **63** 011401
- [5] Puertas A M, Fuchs M and Cates M E 2002 *Phys. Rev. Lett.* **88** 098301
- [6] Foffi G, Dawson K A, Buldrey S V, Sciortino F, Zaccarelli E and Tartaglia P 2002 *Phys. Rev. E* **65** 050802
- [7] Zaccarelli E, Foffi G, Dawson K A, Buldrey S V, Sciortino F and Tartaglia P 2002 *Phys. Rev. E* **66** 041402
- [8] Mallamace F, Gambadauro P, Micali N, Tartaglia P, Liao C and Chen S H 2000 *Phys. Rev. Lett.* **84** 5431–4

- [9] Pham K N, Puertas A M, Bergenholtz J, Egelhaaf S U, Moussaïd A, Pusey P N, Schofield A B, Cates M E, Fuchs M and Poon W C K 2002 *Science* **296** 104–6
- [10] Eckert T and Bartsch E 2002 *Phys. Rev. Lett.* **89** 125701
- [11] Chen S H, Chen W-R and Mallamace F 2003 *Science* **300** 619–22
- [12] Pontoni D, Narayanan T, Petit J M, Grübel G and Beysens D 2003 *Phys. Rev. Lett.* **90** 188301
- [13] Grandjean J and Mourchid A 2004 *Europhys. Lett.* **65** 712–8
- [14] Sciortino F 2002 *Nat. Mater.* **1** 145
- [15] Manley S, Wyss H M, Miyazaki K, Conrad J C, Trappe V, Kaufman L J, Reichman R and Weitz D A 2005 *Phys. Rev. Lett.* **95** 238302
- [16] Lu P J, Conrad J C, Wyss H M, Schofield A B and Weitz D A 2006 *Phys. Rev. Lett.* **96** 28306
- [17] Zaccarelli E, Sciortino F, Buldyrev S V and Tartaglia P 2004 *Short-Ranged Attractive Colloids: What is the Gel State?* (Amsterdam: Elsevier) pp 181–94
- [18] Foffi G, De Michele C, Sciortino F and Tartaglia P 2005 *Phys. Rev. Lett.* **94** 078301
- [19] Stradner A, Sedgwick H, Cardinaux F, Poon W C K, Egelhaaf S U and Schurtenberger P 2004 *Nature* **432** 492–5
- [20] Baglioni P, Fratini E, Lonetti B and Chen S H 2004 *J. Phys.: Condens. Matter* **16** S5003–22
- [21] Campbell A I, Anderson V J, van Duijneveldt J and Bartlett P 2005 *Phys. Rev. Lett.* **94** 208301
- [22] Sciortino F, Mossa S, Zaccarelli E and Tartaglia P 2004 *Phys. Rev. Lett.* **93** 055701
- [23] Coniglio A, De Arcangelis L, Del Gado E, Fierro A and Sator N 2004 *J. Phys.: Condens. Matter* **16** S4831–9
- [24] Imperio A and Reatto L 2004 *J. Phys.: Condens. Matter* **16** 3769
- [25] Mossa S, Sciortino F, Tartaglia P and Zaccarelli E 2004 *Langmuir* **20** 10756–63
- [26] Sciortino F, Tartaglia P and Zaccarelli E 2005 *J. Phys. Chem. B* **109** 21942–53
- [27] Wu J, Liu Y, Chen W R, Cao J and Chen S H 2004 *Phys. Rev. E* **70** 050401
- [28] Liu Y, Chen W R and Chen S H 2005 *J. Chem. Phys.* **122** 044507
- [29] Wu J and Cao J 2005 *J. Phys. Chem. B* **109** 21342–9
- [30] Tarzia M and Coniglio A 2005 *Preprint cond-mat/0506485*
- [31] Speedy R J and Debenedetti P G 1994 *Mol. Phys.* **81** 237
- [32] Speedy R J and Debenedetti P G 1996 *Mol. Phys.* **88** 1293
- [33] Zaccarelli E, Buldyrev S V, La Nave E, Moreno A J, Saika-Voivod I, Sciortino F and Tartaglia P 2005 *Phys. Rev. Lett.* **94** 218301
- [34] Zaccarelli E, Saika-Voivod I, Buldyrev S V, Moreno A J, Tartaglia P and Sciortino F 2006 *J. Chem. Phys.* **124** 124908
- [35] Saika-Voivod I, Zaccarelli E, Sciortino F, Buldyrev S V and Tartaglia P 2004 *Phys. Rev. E* **70** 041401
- [36] Götze W 1991 *Liquids, Freezing and the Glass Transition* (Amsterdam: North-Holland) pp 287–503
- [37] Zaccarelli E, Foffi G, Sciortino F, Tartaglia P and Dawson K A 2001 *Europhys. Lett.* **55** 157–63
- [38] Sciortino F and Kob W 2001 *Phys. Rev. Lett.* **86** 648–51
- [39] Zaccarelli E, Foffi G, Dawson K A, Sciortino F and Tartaglia P 2001 *Phys. Rev. E* **63** 031501
- [40] Zaccarelli E, Foffi G, Dawson K A, Buldyrev S V, Sciortino F and Tartaglia P 2003 *J. Phys.: Condens. Matter* **15** 367
- [41] Sperl M 2003 *Phys. Rev. E* **68** 031405
- [42] Zaccarelli E, Foffi G, Sciortino F and Tartaglia P 2003 *Phys. Rev. Lett.* **91** 108301
- [43] Zaccarelli E, Sciortino F and Tartaglia P 2004 *J. Phys.: Condens. Matter* **16** 4849–60
- [44] Sciortino F, Tartaglia P and Zaccarelli E 2003 *Phys. Rev. Lett.* **91** 268301
- [45] Götze W and Sjögren L 1987 *Z. Phys. B* **65** 415